



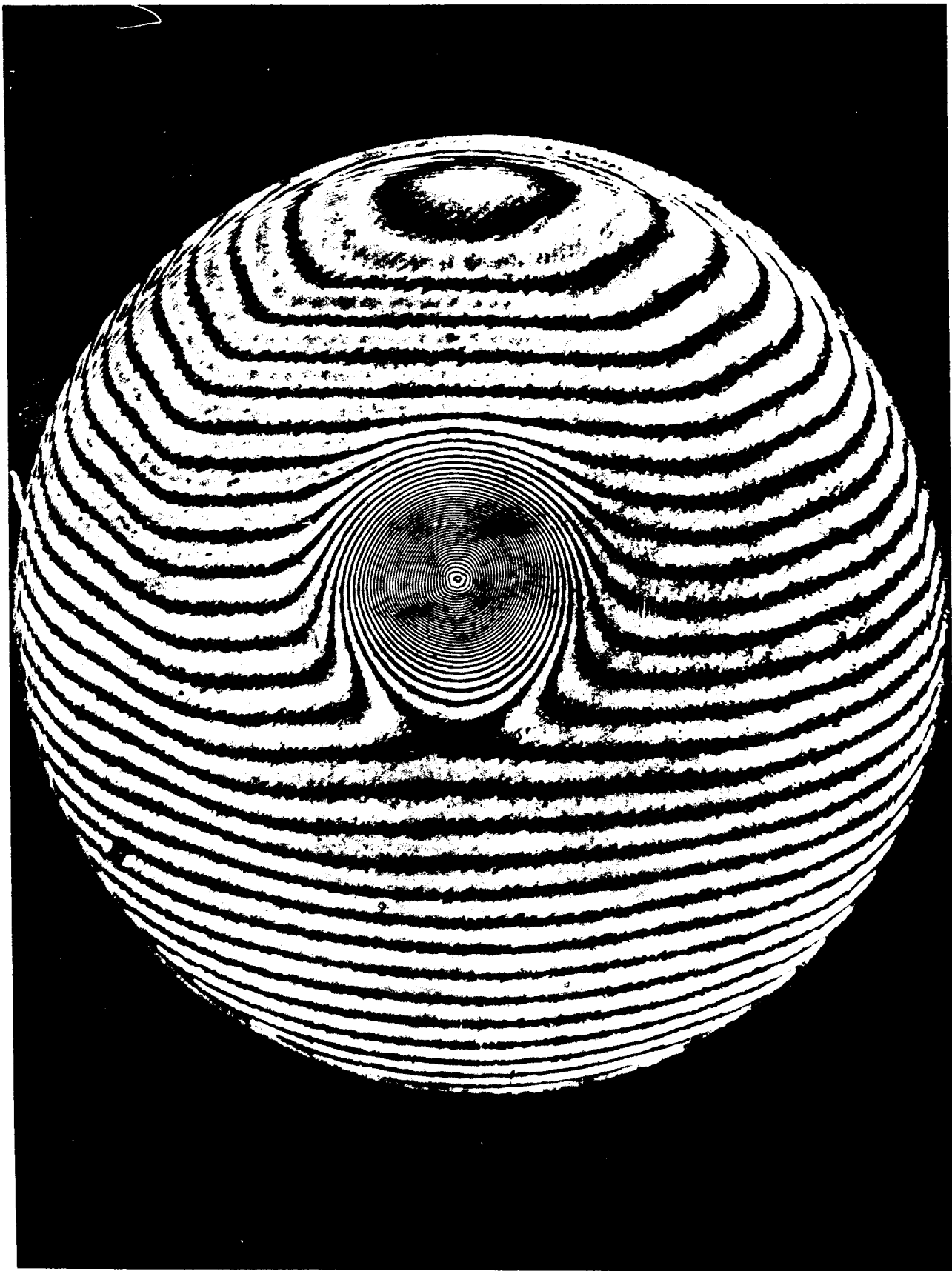
LA-5058-MS
Informal Report
UC-37

ISSUED: October 1972

Holographic Interferometry Cookbook

by

F. C. Jahoda
R. E. Siemon



HOLOGRAPHIC INTERFEROMETRY COOKBOOK

by

F.C. Jahoda and R.E. Siemon

ABSTRACT

Various approaches to pulsed holographic interferometry are described and our reasons are given for preferring non-diffuse holograms which contain on the hologram an image of the plasma. Many details often omitted from more formal publications are given concerning laser requirements, optical components, recording materials, and so on. A discussion is given of the interpretation of plasma interferograms in which it is emphasized that interferometric data is very useful quantitatively as well as qualitatively.

I. INTRODUCTION

The development about ten years ago of the giant pulse ruby laser furnished plasma physicists with a light source that is sufficiently bright, monochromatic, directional, and of short duration to enable "stop-action" space-resolved interferograms of highly self-luminous, transient plasma discharges to be made relatively easily. These lasers were also coherent enough so that the tedious path length matching procedures required of interferometers with conventional light sources were sufficiently relaxed to permit alignment by non-specialists with a modicum of patience.¹

A significant subsequent simplification was the switch to holographic interferometry. In its simplest conceptual form this is an overlay (double exposure) of two very fine scale interferograms made sequentially to produce a coarser fringe pattern (Moire' beats) which delineates contours of constant (odd multiples of π) phase change between the two exposures (e.g., by the introduction of a plasma) analogous to the conventional interferometer fringe structure. The relative uniformity of each individual fine scale interferogram is of no concern, since only the constancy of the pattern, aside from those deliberate changes which are the object of the measurement, is required. Thus, merely by placing some-

what stricter requirements on a) the laser coherence (in order to be able to produce fine scale fringes of high order number) and b) the resolution capability of the photographic plate detector (in order to record the fine scale fringes) one can dispense both with the expensive high optical quality interferometer, e.g., Mach-Zehnder, itself and its attendant restraints on the physical configuration of the plasma device, as well as the high optical quality generally needed for components between the interferometer beam splitters - e.g., plasma vessel windows.

Although the principles of holography are by now widely known and well documented,² we attempt in this report to describe the numerous small details of operational procedure and degrees of flexibility that we have learned over the years. Many of these are relatively obvious and others can undoubtedly be improved upon. Nonetheless holographic interferometers can be usefully adapted in such a wide variety of circumstances that we have found ourselves questioned on these details over and over. Therefore it seems worthwhile to attempt to summarize them in this report.

II. APPLICABILITY OF HOLOGRAPHIC INTERFEROMETRY

An absolutely essential prerequisite before

attempting ruby laser holographic interferometry would seem to be an estimate of whether the anticipated refractivity change between the two exposures falls within the sensitivity range of the method.

The refractive index of a fully ionized plasma is dominated by the electron refractivity, μ . The fringe displacement, p , due to the substitution of plasma for vacuum (or to very good approximation neutral gas) in units of fringes is $\int_0^L (\mu-1) d\ell/\lambda$

where $d\ell$ is the element of path length along a ray, L is the plasma length, and λ is the wavelength of the laser radiation. From the dispersion relation of a transverse electromagnetic wave in a cold, field-free plasma, $k^2 = (\omega^2/c^2) (1 - \omega_p^2/\omega^2)$, where ω is the angular frequency of the radiation, $\omega = 2\pi c/\lambda$, and ω_p is the plasma frequency, defined by $\omega_p^2 = \frac{4\pi n e^2}{m}$, and using the definition of the refractive index, $\mu = \frac{ck}{\omega}$, one obtains the fringe shift:

$p = nL/3.2 \times 10^{17}$ for $\lambda = 6943 \text{ \AA}$, where n is the electron density in cm^{-3} , length is measured in centimeters, and we have replaced the integration by the product of average density times length.

It will be demonstrated in a following section that fringe displacements between 1/10 and 30 fringes per centimeter, given at least a 1 cm^2 cross-section transverse to the laser beam, can be readily measured. (These are not fundamental limits and could be extended in both directions by careful technique). These fringe displacements then define the doubly cross-hatched area on the n, ℓ plane in Fig. 1, with the upper boundary flattening at $n = 10^{19} \text{ cm}^{-3}$ for $\ell < 1 \text{ cm}$, since it is unrealistic to assume a larger cross-section than depth dimension. Likewise it becomes increasingly difficult to measure fractional fringes as the cross-section decreases below 1 cm (since fractional fringes are sensed as distortions in an array of a finite number of fringes) and the lower limit of 1/10 fringe is gradually increased to the 1 fringe displacement line for $\ell < 1$.

Outside the cross-hatched region ruby holographic interferometry is not directly applicable, but certain special measures in some instances may in effect move the actual n, ℓ coordinate into the cross-hatched area. For instance, if the length is reasonable but the density is too low, a multiple

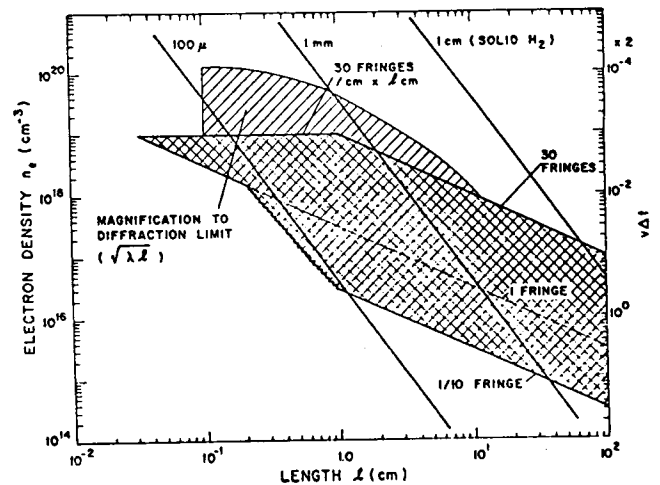


Fig. 1. Approximate range of applicability for ruby laser interferometry.

path scheme (generally at the expense of space resolution) effectively increases n by a factor equal to the number of traversals. (A note of caution, however: Nothing is gained if the smallest detectable fringe shift (noise level) is increased by the same factor, as can easily occur, unless elaborate special experimental means are taken to avoid this). For a point to the upper left of the graph, i.e., sufficiently dense that the actual $n\ell$ product exceeds, say, the 1 fringe level of 3×10^{17} but the length is too small to fall into the cross-hatch area, (e.g., plasma focus or laser produced plasma) optical magnification to a lateral dimension compatible with the depth dimension of the diagram effectively slides the point along an $n\ell = \text{constant}$ diagonal. If the plasma is of sufficient length but so dense that fringes crowd together too much to be resolved, magnification of the test section can extend the accessible range, as shown by the top shaded

$$\mu^2 = 1 - \frac{\omega_p^2}{\omega^2}$$

area. The limit on magnification is taken to be that factor which increases the diffraction limited resolvable distance to 1.30 cm. This diffraction limit d is assumed to be $d = (\lambda l)^{1/2}$, obtained from the diffraction angle $\theta \approx \lambda/d$ spreading to a size d over distance l . Another limit on resolution is given by the bending of the laser light in the refractive index gradient, but this effect increases with l^2 and only becomes dominant in the region off the graph to the right.

For reference, three lines are plotted indicating the density vs length relationship during uniform spherical expansion of solid hydrogen pellets of three different initial radii. An additional constraint is placed on the duration of the laser pulse by the requirement that the nl product change by less than $1/8$ fringe during the laser exposure. The extra scale on the left gives the maximum product of pulse duration times uniform spherical expansion velocity that still fulfills this criterion.

For small nl products an attractive possibility is to increase the laser wavelength, since the gain in sensitivity scales directly with wavelength. The $10.6\text{-}\mu$ CO_2 laser is a natural choice, but the problem of a detector with enough sensitivity and sufficiently high-spatial resolution is not yet very well in hand and outside the scope of this report. (Note also that $10.6\text{-}\mu$ radiation is not transmitted by Pyrex or quartz).

III. CONFIGURATIONS

A. Diffuse Scene Beam (Diffuse Hologram)

The method most nearly analogous to the ordinary diffuse reflection holography of opaque objects, and historically, the first holographic interferometry method for plasmas used by us,³ interposes a ground glass diffuser (sandblasted slide cover) in the scene beam upstream of the plasma. Each single diffuser point then illuminates (through the plasma) every point of the photographic plate. If the diffused light is weak relative to the collimated reference beam, the intermodulation terms (interference between different scattering points) are of second order, and the fine scale interference structure can be thought of as an overlay of Fresnel zone plates, one for each independent scattering point of the diffuser. The resulting spatially jumbled exposure pattern on the photographic plate can then be un-

scrambled by reconstruction with collimated, monochromatic (most conveniently, gas laser) light, with each Fresnel zone plate acting as a lens having both real and virtual foci at fixed spatial locations according to the effective center and scale length of the ring structure on the developed plates. Double exposure, as in the overlap of straight fringes, destroys the interference structure selectively for those locations where there is a phase change of an odd multiple of π between exposures, giving the equivalent of conventional fringes in the reconstructed image of the diffuser.

Because the phase differences of interest are generated in a space that may be a considerable distance in front of the diffuser, the scheme just outlined can work only if the solid angle through which the diffuser is viewed at any one time in the reconstruction is sufficiently restricted that the 2-exposure phase difference along a given line of sight to a given point on the diffuser is not "washed out" by a different line of sight to the same point of the diffuser. By the same token by deliberately changing the restricted direction cone through which a given hologram is viewed the fringe structure will change according to the phase differences along the viewing directions, and inferences about the depth dimension (integrated along for any single direction) can be made.

In practice we have found that the range of directions over which our plasmas can be viewed is in any case so limited by the vessel and coil configuration that we much prefer to give up the three dimensional inference possibility (a complicated unfolding of the various views would still be necessary) in favor of the experimental advantages gained if the diffuser is moved downstream to a position between plasma and photographic plate. These advantages are 1) the reconstruction can be done with relatively large solid angles without washing out the fringe structure and 2) the correct scene beam exposure of the photographic plate, given the finite energy of the laser pulse and a given reference beam intensity can be easily adjusted by choosing the distance between diffuser and plate solely on this basis. (In our typical setups this distance has been of the order of 20 in.) With the diffuser downstream of the plasma, one obtains an interfero-

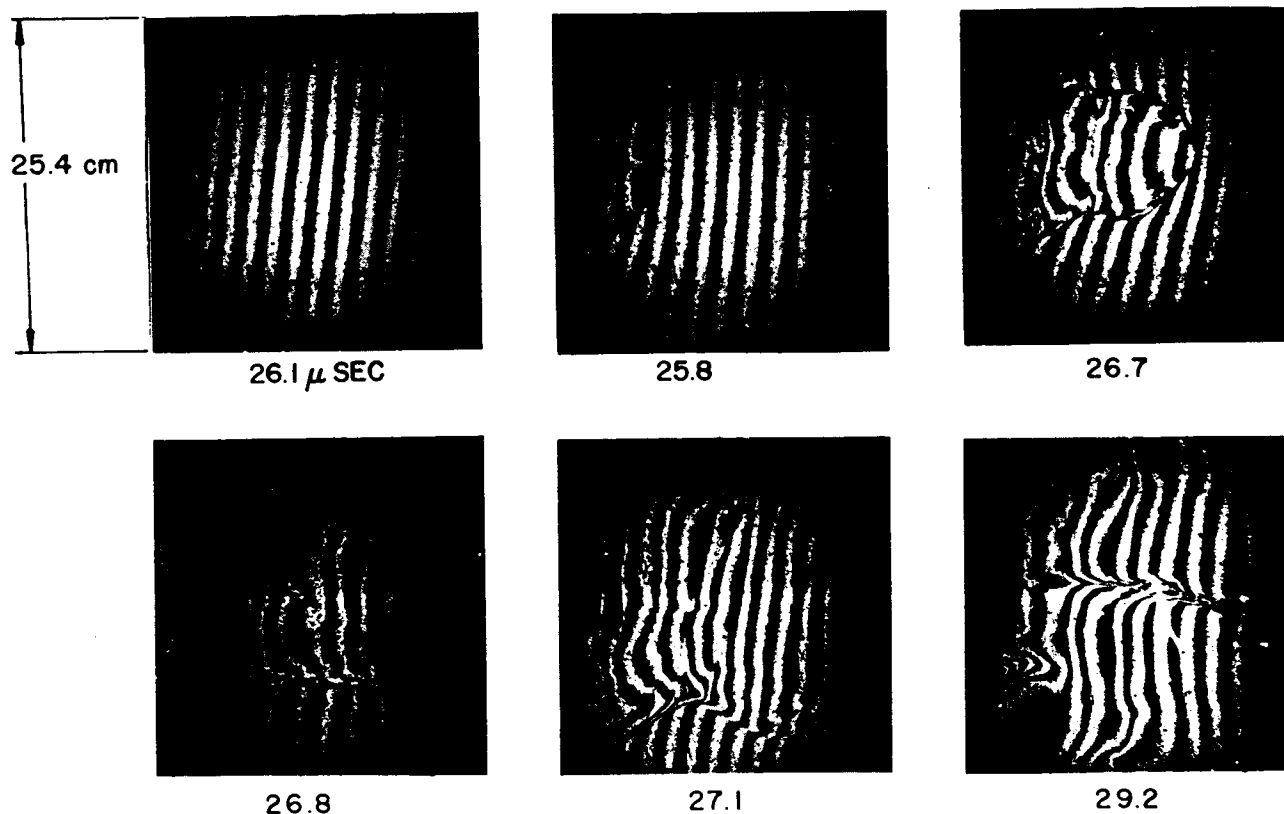


Fig. 2. Large diameter holographic interferograms made with a diffuse scene beam.

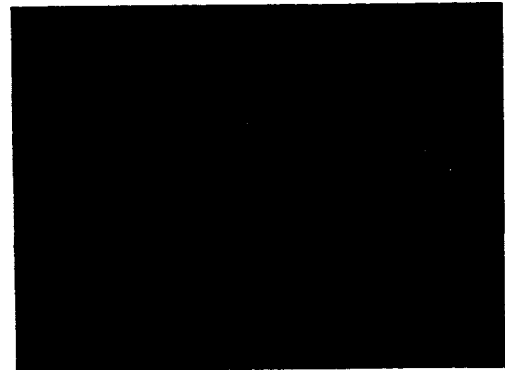
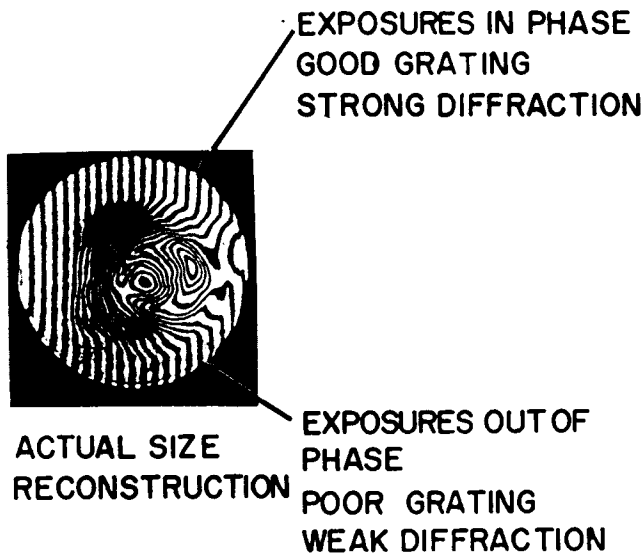
gram corresponding to the direction that the collimated laser light traverses the plasma, independent of the direction in which the diffuser is viewed in reconstruction. In principle, the fringes are localized on the surface of the diffuser. If, however, on occasion there is a relative motion between diffuser and photographic plate during the time between the two exposures, the fringes will be localized in a different plane, and parallel effects are observed between the fringes and diffuser image. Depending on the severity of this effect the reconstruction solid angle may have to be reduced somewhat in this case also, in order to avoid fringe washout. Examples of diffuse holographic interferograms of a coaxial gun neon plasma are shown in Fig. 2. The straight line background fringe structure is discussed in detail below. The test section dimension is 25-cm x 25-cm, which would itself be rather extreme for interferometer optics, and the plasma was in a 6-ft diameter vacuum tank which could not read-

ily have been spanned by a conventional interferometer.

B. Collimated Scene Beam (Image Hologram)

By removing the diffuser in the scene beam entirely, the collimated laser beam projects the test section onto the photographic plate with a one-to-one correspondence between test section and photographic plate. Again, two exposures are made, with and without plasma. This is similar to the old technique of overlaying two interferograms and observing the Moiré beats. The details are illustrated in Fig. 3. We call it an image hologram for the following reasons: 1) we actually image the test section onto the plate with a lens so that to first order the spatial displacement of the projected beam due to strong transverse refractive index gradients (as opposed to the desired phase delays due to changed refractive index along the ray path) is removed and the Moiré beats are overlaid on an area on the photographic plate that is a good

DOUBLE-EXPOSURE HOLOGRAM MADE WITHOUT DIFFUSER (IMAGE HOLOGRAM)



HOLOGRAM MAGNIFIED 320X

Fig. 3. Microphotographs on the right show the effect on the hologram of the double exposure procedure.

image of the test section, 2) every analysis of any kind of holography uncovers a very close relationship to some form of interferometry of which it becomes a special or generalized case and 3) the individual fringe patterns are so dense that we actually use non-zero order diffraction in the reconstruction (as described in detail below) to remove extraneous noise, e.g., coarse fringe structure originating by multiple reflections in either beam alone. Also, as will be demonstrated, by isolating a diffracted order and reimaging the plate we achieve a very large increase in the range of useful exposure level.

The major advantage of the image hologram is that by removing the diffuser one essentially eliminates the familiar speckle pattern always associated

with coherent light on a diffuse surface, and thereby significantly increases the resolution possible when the Moiré fringe pattern becomes dense due to relatively large refractivity changes between exposures. Since the scene and reference beams can, if necessary, be carefully overlapped on the plate (following amplitude division at the original beam-splitter) so that corresponding regions recombine, the spatial coherence requirements on the laser source are further reduced. Although an optical system is used for high quality, bright reconstruction, the fringe structure is localized on the plate and can generally be seen at a glancing angle in ambient illumination rather than requiring a) a laser and b) locating the correct image plane in space.

The bulk of the remainder of this report concerns itself with these nondiffuse image-type

interferograms.

Generally in the recent past we have favored this method over the diffuse hologram method described above, feeling that its disadvantages are considerably more than compensated by the advantages. We consider these in turn.

The major disadvantage of the non-diffuse image hologram is that the only areas of the scene which can be reconstructed are the areas correctly overlapped by the reference beam. This is in contrast to the use of a diffuser which permits the whole scene to be reconstructed from any properly exposed part of the hologram. In practice this is not troublesome since the reference beam is relatively easy to handle. It need not be aligned with any experimental axis and needs no windows. Another disadvantage is that only uni-directional information can be obtained. This was in any case already conceded in the experimentally simpler case of diffuser downstream from the plasma. There may be some advantages to a diffuse image hologram in which a diffuser is placed before the test section and then the test section is imaged on the hologram plate. This would contain features of "image-holography" in which reconstruction (using apertures to select the viewing direction can be accomplished with white light), but we have never tried such a scheme.

At one time we believed that it would be easier to get multiple frame interferograms during a single plasma discharge from the diffuse hologram, e.g., by spatially separating several reference beams, each covering only a small area of plate. However, again as described below, we have gotten three frames of good quality with the non-diffuse image holograms. Specialized simple geometries e.g., such as the "scatter plate" beamsplitter where the reference beam is never really separated far from the scene beam, are intrinsically dependent on the nature of the diffuser. A nice example of this is seen in laser produced plasma work at Garching.⁴

C. Multiple-Frame Interferograms

If the individual events to be studied are expensive of time and/or money or, as in the case of developing instabilities, not accurately reproducible from shot-to-shot, it is desirable to obtain a time sequence of interferograms during a single

event. In conventional interferometry this can be achieved with some form of image transport - e.g. streak or framing camera, provided only one has an illumination source of sufficient time duration. In holographic interferometry, however, one also requires accurate registry (to fractional wavelengths) of two exposures, one before and one during the event, for each frame and this precludes simple streak or framing methods. Two quite different means of achieving multiple frames are described below.

1. "Live Fringe" method. This is an adaptation of a method sometimes used in CW laser holography to study slow changes in real time. Instead of two consecutive exposures of the hologram emulsion that yield a permanently recorded beat pattern on the emulsion, the hologram is photographically processed after a single exposure of the passive state before the plasma event and then accurately repositioned. Whenever the laser illumination source is again turned on, e.g. during the plasma event, interference occurs in real time between a) the stored virtual image of the passive scene, reconstructed in first order by the beam that was the reference beam in the holographic recording, and b) the current status in the scene beam, directly transmitted in zero order. Consecutive interferograms can then be photographed by image convertor cameras gated on at pre-selected times.

Interference fringes will occur both because of the phase changes in the scene that one wishes to measure and because of inexact repositioning of the hologram. However, by mounting the photographic plate in a repositionable jig that goes through the development process, the residual phase shift of the repositioning error is slight, and moreover, small compared to the linear phase shift deliberately introduced between exposures to give a background of straight fringes. This alters only slightly the orientation and spacing of the background in a harmless manner.

A demonstration of this method, using a giant pulse laser to make the hologram and for the interferogram formation, a chilled free-running ruby laser of lesser coherence (mirrors coated directly on the ruby rod) is given in Ref. 5. A source of multiple giant pulses could of course also be synchronized with the image convertor frames. One distinction then from the multiple pulse method to be

discussed immediately below is the fact that no spatial separation is needed between successive reference beams. The resolution requirement of the electro-optic detector device need only be that required for the display of the final result interference pattern, and not the high resolution of the holographic recording medium. This, however, can still be a severe requirement if a high fringe density needs to be displayed, and is the principal reason why we have chosen to pursue the following alternative method. The live fringe method, however, has the advantages of almost real time read-out and being easily adaptable to remote read-out via closed-circuit television.

2. Multiple Laser Sources. If an appropriately timed sequence of giant pulse lasers is available and a diffuser is included in the scene beam, one can simply utilize a hologram's ability to store independently several (double) exposures by spatially separating relatively small areas of the emulsion exposed by the individual reference beams. (The separation can also be angular rather than spatial if a sufficiently thick emulsion is used). This is readily done by means of passive beam splitter elements if the various pulses originate at separate spatial points. On the other hand, if the multiple source is a time sequence from a single laser, some active element (e.g. rotating mirror or electro-optic beam deflector) is required, and this complicates the arrangement.

More surprising, perhaps, is that with three lasers we have been able to retain the advantages of the non-diffuse image hologram method by splitting the scene beam into three distinct beams with a transmission grating after it has traversed the region of interest (Fig. 4). Each of the three separated scene beams, which consist of three consecutive pulses, is then combined on a separate photographic plate with one reference beam, coherent according to its origin with, respectively, one of the scene beams. After a double exposure (two firings of each of the three lasers) one obtains on each plate the usual holographic interferogram overlaid with four extra non-coherent exposures from the other two scene beams. Particularly after bleaching this additional exposure is of no consequence and the final reconstructed result (Fig. 5) is of comparable high quality to the single frame

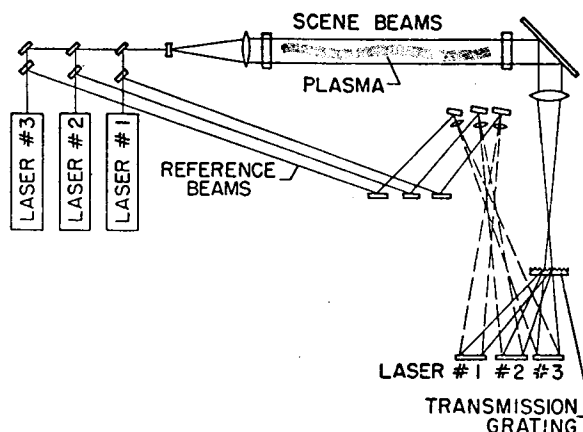


Fig. 4. Schematic arrangement of 3-frame holographic setup. Note that reference beams are not expanded until necessary at the holographic plates.

image hologram.

IV. DESIGN CONSIDERATIONS

A basic one-laser non-diffuse or image hologram arrangement is shown schematically in Fig. 6. Most of the discussion in this section concerns results obtained with this system except that the 6943 Å interference filter was found unnecessary when using Agfa-Gavert plates.

A. Pulsed Ruby Laser Requirements

In recent years very good quality holographic lasers have become available from various companies. The basic requirements are spatial and temporal coherence. Korad holographic lasers, with which we are most familiar, typically offer a TEM_{00} output of 50 mJ in a 1-2 mm beam and a coherence length of over 50 cm.

The most important ingredient is a carefully selected ruby, i.e., one free of optical inhomogeneities. Also, an innovation which has improved lasers for holography is the inclusion of an aperture inside the lasing cavity. It can be shown that due to diffraction the gain for lasing in the TEM_{00} mode relative to the gain for any higher mode becomes larger as one reduces the transverse dimension of the cavity. In the lasers we use, the beam is 1.5 or 2.0 mm in diameter as defined by a hole in a metal aperture.

In double-exposure holographic interferograms the effects of laser coherence can be subtle and difficult to understand. When one introduces a

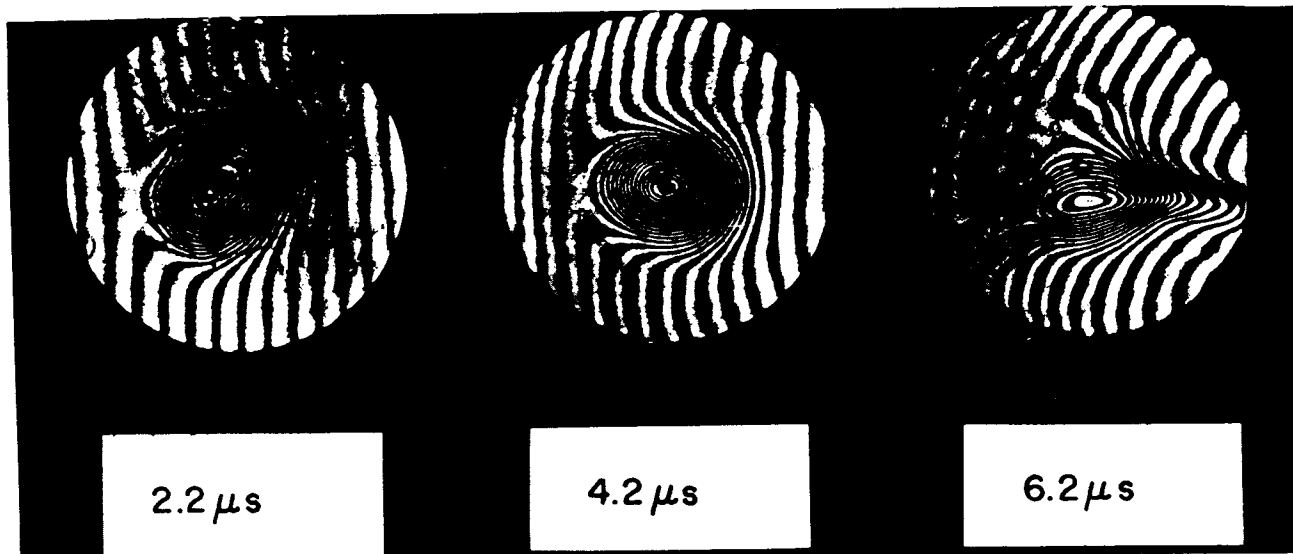


Fig. 5. Time sequence of holograms showing the development of an instability at low temperatures.

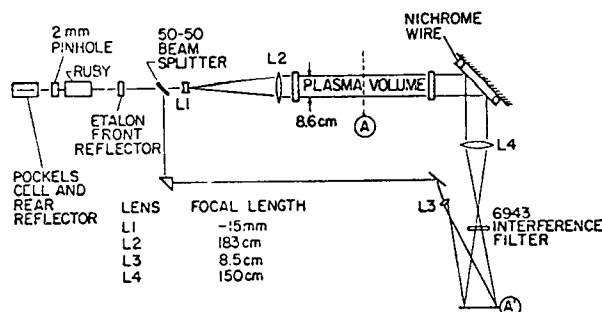


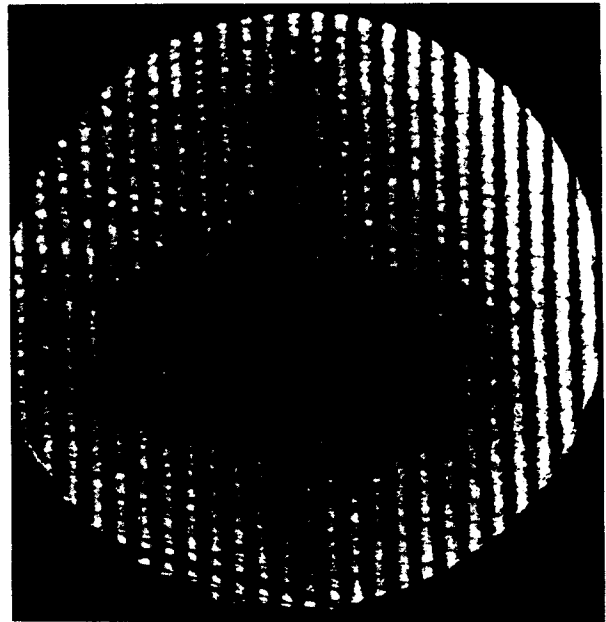
Fig. 6. Schematic arrangement for recording non-diffuse holograms. Lens L4 images plane A onto A' to minimize refractive effects. The reference beam is not expanded except by diffraction until it reaches lens L3.

uniform variation between exposures such as by tilting a mirror, the result can be crooked or wavy fringes which in some instances can even split. Figure 7 shows examples of double-exposure interferograms made in nearly identical image-hologram configurations but with different lasers. In each case a mirror was tilted between exposures. The "old laser" contained a ruby purchased in about 1966 and had an external 1 mm pinhole. The "new laser" had a 1.5 mm internal pinhole and was purchased in 1969. Interferograms of the ruby rods showed as many as 11 fringes (6328A) on the old rod and less than 2 on the new rod.

Certain artifacts about these pictures are ignorable. The Allen wrench in the field of view of the old laser was an alignment aid. Imperfections such as lines diagonal to the fringe pattern and circular fringes on the edge are directly traceable to imperfections like scratches in windows and diffraction of the scene beam at its edge. They appear to the eye when viewing the scene beam in alignment laser light and naturally are present in the hologram.



"OLD" LASER



"NEW" LASER

Fig. 7. Comparison of double-exposure holograms made with a good (new) and bad (old) ruby rod. Fringes are obtained by tilting a mirror between exposures.

The important differences are in the fringe quality. The waviness of fringes from the old laser is apparent and a split fringe, for example, can be found by coming up from the bottom, about three fringes to the left of center.

Another important difference is the uniformity of playback brightness. The plate exposure on these two holograms was approximately equally uniform. Clearly however, the old laser did not make a uniform hologram.

Certainly not everything is known about the difficulties seen on the old laser result but one interesting experiment with the new laser suggests the trouble is not predominantly due to temporal coherence (*i.e.*, coherence length). The experiment consisted of monitoring the line structure of the new laser output with a Fabry-Perot interferometer while making interferograms like those in Fig. 7. By varying the temperature of the front reflector of the laser cavity, which is itself an etalon to provide longitudinal mode selection, it was possible to observe a variety of longitudinal mode structures and compare the resulting interferograms.

The laser mode drifted from a single line about $.02 \text{ \AA}$ wide to a double line of equal intensity separated by about 0.1 \AA . (A separation of 0.1 \AA corresponds to a beat every 10 cm). However, the resulting interferograms showed no apparent difference in brightness, uniformity, or fringe structure. This is not surprising since a holographic interferometer does not require a large continuum of path lengths over which interference occurs as in, for example, a diffusely illuminated scene of varying depths. If, however, the relative phase differences over the ruby cross-section were different for the two exposures, wavy and split fringes can be explained. The conclusion is apparently that spatial coherence provided by the rod quality and internal pinhole is more important than coherence length for holographic interferometry.

A trick which helps when working with nondiffruser holograms and a poor laser is to expand the beam before splitting the reference from the scene beam. Then with care one can recombine the scene and reference beams so that point by point they are superimposed. In this way the need for spatial

coherence is greatly relaxed.

In all, the message to be conveyed is that a good quality laser is a great asset.

B. Choice of Optical Components and Physical Layout

One of the attractive features of holographic interferometry is the freedom to use ordinary optical components while making measurements accurate to a fraction of a wavelength. This is possible because the double-exposure procedure makes a comparison of the same scene at two times.

There is one important reservation. Since the scene beam consists of collimated light going often-times over long paths, it is necessary to use care in selecting and arranging components to uniformly illuminate the region of interest and to relay the illumination to the hologram. Put more simply, if you don't have a good scene beam you can't have a good interferogram. Windows which seem fairly good to the eye can appear very poor when viewed in collimated light due to bunching of rays caused by small imperfections.

If one is forced by the experiment to use poor windows it is very helpful to image the scene onto the hologram plane. Figure 8 shows schematically what is involved. If the windows are good enough to "see through" they may still destroy a collimated beam after it propagates a distance. A lens, like the eye, can untangle the rays whatever their direction and restore them to their proper location providing of course, the distortion isn't so bad that the rays miss the lens. It further provides each ray with exactly the same optical path length it would have had if it had gone straight (which is why it is a lens, if you think of it that way). If the windows are too bad for this trick you essentially cannot see through them.

The reference beam when working with a diffuser may be shoddy since any part of it will provide a reconstruction. Without a diffuser one has to be more careful although it is usually easy to handle the reference beam since it does not have to be expanded until it reaches the hologram plate.

In practice we find very inexpensive components such as lenses and mirrors from Edmund Scientific are adequate for most purposes. Figure 9 shows Polaroid pictures of scene and reference beam intensity as they arrive on the holographic plate.

Inexpensive components can be interchanged, rotated, etc. until satisfactory results are obtained. With a carefully aligned gas laser, all features of the scene and reference beam are visible in alignment laser light. Kodak neutral density filters are frequently used to adjust beam intensity.

Dielectric, glass and pellicle beam splitters have all been used. Silvered glass is not advisable for use in an unexpanded beam where the power per unit area can be large. Multiple reflections from components can be a problem which we try to avoid by tilting or careful placement rather than anti-reflection coatings which tend to wear out. Multiple reflections at the beam splitter are easily avoided by splitting the beam with thick uncoated glass as shown in Fig. 10. Picking off a weak

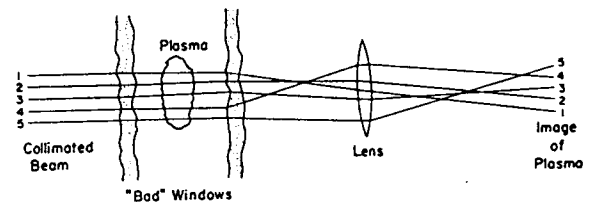


Fig. 8. Showing the effect of bad windows and how a lens in the scene beam can help correct distortions.

reference beam while delivering it with equal intensity at the hologram is possible since the scene beam needs to be expanded and is often attenuated more by its optics. For example, a uniform scene beam is most easily obtained if one expands the beam to two or three times its final size and uses the center portion.

Vibrations are often feared in double-exposure applications since it takes time to recharge a laser for the second exposure. Of course our reference exposure is routinely recorded before the plasma shot so that the magamp discharge has no time to

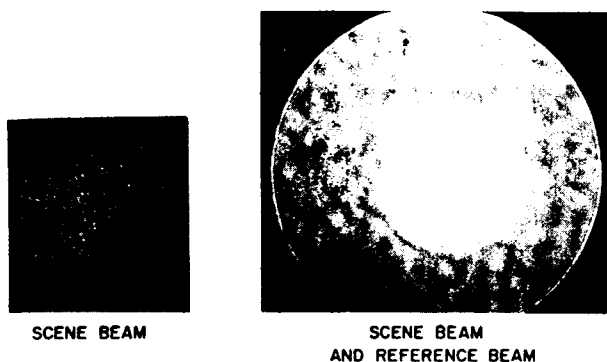


Fig. 9. Polaroid pictures of scene and reference beams as they arrive on the hologram plate. Appearance of gas alignment laser is essentially the same.

cause mechanical effects. Still it is true that the scene beam optical pathlength is compared to a fraction of a wavelength of light at two instances separated by as much as several minutes. This seems troublesome until one realizes that many motions such as moving a window slightly have no leading order effects and other motions such as tilting a mirror simply add to the already uniform and more or less arbitrary background pattern of straight fringes (see part E of this section). It has been our experience that vibrations are easy to avoid and seem to present no problem in holographic interferometry so long as no quivering or shaking can be seen in alignment laser light.

It should be briefly mentioned that carefully mounting and aligning a He-Ne alignment laser is time well spent. We mount the He-Ne laser on the ruby laser bench with a turning mirror which is removable and uses three fixed 1/4" ball bearings and a proper three point support scheme for accurate repositioning.

The final point is that getting attractive interferograms is more a matter of patience, trial-and-error, and to some extent, experience than a matter of holographic subtleties. When the holography is done perfectly it can do no more than record the scene beam created by the experimenter.

C. Recording Materials and Techniques of Processing.

Table I lists a number of products with which we have experience. By far the most frequently used has been Agfa-Gavert 10E75.

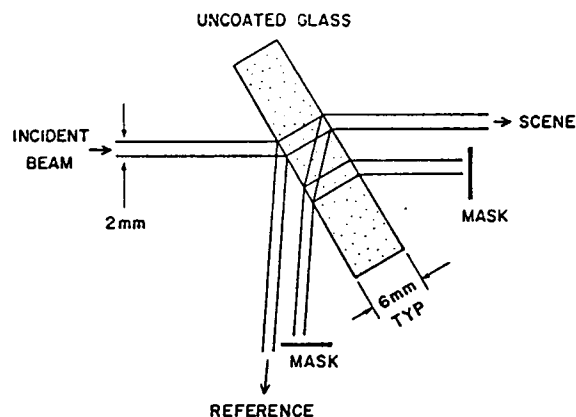


Fig. 10. One possible arrangement to separate scene and reference beam with no secondary reflections.

With image holograms we have adopted the following technique:

1. Provide rather heavy double-exposure.
2. Develop in Kodak HRP developer for 5 minutes ($72 \pm 5^\circ \text{F}$).
3. Fix(Kodak Rapid Fix) for 5 minutes.
4. Rinse in running water 2 minutes.
5. Bleach in Kodak Chromium Intensifier mixed with 2/3 the amount of water called for on directions (it helps to mix with hot (110°F) water) until plate is uniformly yellow.
6. Rinse about 1 minute in water.
7. Rinse in clearing bath (comes with chromium intensifier and mixed as recommended) until yellow goes away - about 2 minutes.
8. Wash in running water 10 minutes.
9. Dip in Kodak Photo-Flo for 30 seconds.
10. Allow to dry.

The process is certainly not critical and our attempts to optimize various details have shown that results are insensitive to variations.

The bleaching process gives such a greatly enhanced playback brightness that the interferogram fringes on the hologram are readily apparent to the eye. Bleaching has a much less pronounced effect on diffuse holograms although playback brightness can be increased. A bleached hologram slowly darkens under fluorescent lights but can be rebleached with no obvious effects. We usually save the finished plates in 4 x 5 manila envelopes designed to hold negatives.

TABLE I
Materials for Recording Holograms

Material	Approximate required exposure and available resolution		Comments
1. Kodak 649-F	1.5×10^5 erg/cm ²	3000 lines/mm	Too insensitive for most applications.
2. Kodak SO-243	10^3 erg/cm ²	600 lines/mm	No longer available but used extensively in early work.*
3. Agfa-Gavert 10E75	40-80 erg/cm ²	2800 lines/mm	Exposure is that needed for a 10-50 ns pulsed laser.
4. Agfa-Gavert 8E75	150-300 erg/cm ²	3000 lines/mm	Exposure is that needed for a 10-50 ns pulsed laser.
5. Hughes Photopolymer	10^3 erg/cm ²	1000-3000 lines/mm	See text for comments.

*Kodak has research in progress which may lead to better materials than these listed but no products are available at this time.

The exposure for image holograms is best when scene and reference beams are of equal intensity. For diffuse holograms it is best to make the ratio of reference to scene beam about 10:1. The total exposure for image holograms has an incredible range of well over two orders of magnitude. Figure 11 shows the playback of a hologram with exposures which vary by a factor of twenty and an exposure 5 times stronger (no N.D.) was even better. The washout apparent in the most weakly exposed regions is partly due to the exposure chosen for reconstruction. This latitude is one of the attractive features of the non-diffuser configuration. Incidentally, a reasonable laser intensity for exposing 10E75 is very roughly that necessary to expose 3000 speed Polaroid (very insensitive at 6943 Å) with N.D. 0.7 in front of it.

Included in the table of materials is an in-place, dry-processing photopolymer developed at Hughes Research Laboratories.⁶ Its use eliminates the photographic processing of every holographic exposure. It is used by mixing two solutions, each of long shelf life when unmixed, within one hour before exposure, spreading the mixture between glass plates to approximate a photographic plate, and finally pre-exposing the chemicals slightly to remove certain initial inhibitors to the photochemical reaction. It fixes in place by weak uni-

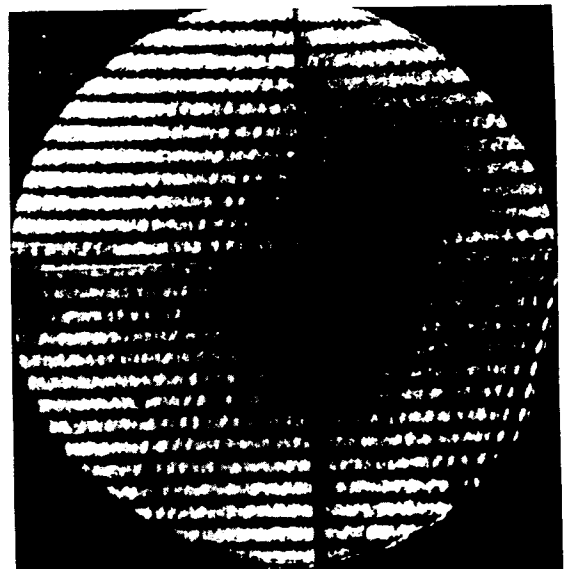


Fig. 11. Showing a reconstructed hologram exposed with four values of neutral density in front of the plate (ND 0.7, 1.0, 1.3, and 2.0).

form ambient light or if desired from UV exposure. Figure 12 is a copy of a polaroid print produced insitu immediately after a plasma experiment using a simply arranged playback scheme. Although the



Fig. 12. Reconstruction of a plasma hologram made with photopolymer

signal-to-noise ratio is worse than with photographic emulsions and the process requires some preparation, the advantages of immediate results are worth considering. It would also be convenient for a method requiring repositioning such as the consecutive frame "live" fringe method.

D. Reconstruction.

Diffuse holograms require monochromatic light for reconstruction. Since it is usually convenient to reconstruct with He-Ne laser light and since the geometry is not necessarily the same in formation and reconstruction, we will record a few useful formulas which help to determine the image locations.

Figure 13 shows the hologram formation with a reference beam which diverges from a point located a distance Y_1 from the hologram. Note the origin of X_1 and Y_1 is the hologram and light is propagating from left to right. Upon reconstruction with wavelength λ' the hologram acts much as a lens with focal length F given by

$$\frac{1}{F} = \left(\frac{\lambda'}{\lambda} \right) \left(\frac{1}{X_1} - \frac{1}{Y_1} \right).$$

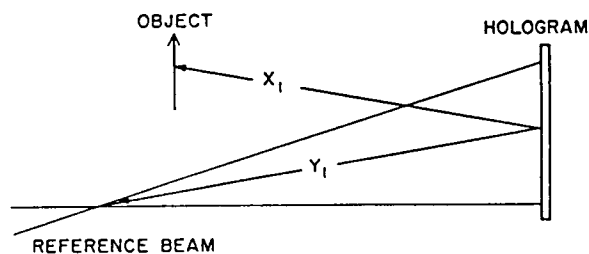


Fig. 13. Notation and sign convention for locating an object in the creation of a hologram made with wavelength λ . In non-diffuse holograms the focus point of the scene beam can be taken as the "object".

In reconstruction with a reference beam at Y_2 as shown in Fig. 14, there will be images at two locations X_2 given by

$$\frac{1}{F} = \pm \left(\frac{1}{X_2} - \frac{1}{Y_2} \right)$$

$X > 0$, image virtual

$X < 0$, image real.

Image holograms can be reconstructed with white light as shown in Fig. 15. If the scene and reference beams are plane waves the hologram is a simple plane-ruled transmission grating. The procedure consists of imaging the hologram onto film using diffracted light for illumination.

When during formation, the scene and reference beams actually diverge from finite distances, the spectrum in reconstruction can be located with the formulas used above by letting X_1 locate the point of divergence for the scene beam and X_2 locate the spectrum.

When an image hologram is viewed in ambient light the Moiré pattern is easy to recognize. If a contact print is made directly from the hologram plate it is possible to discern the plasma fringes, but a reconstruction process such as that in Fig. 15 is far superior to the contact print. The fringe

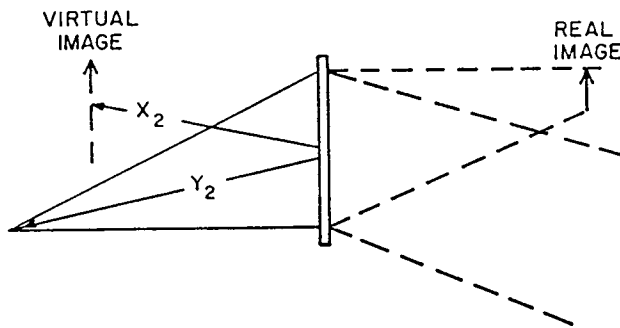


Fig. 14. Notation and sign convention for reconstructing a hologram with wavelength λ' . Light propagates from left to right in this and Fig. 13.

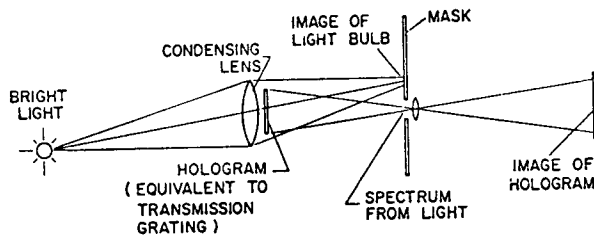


Fig. 15. White light reconstruction scheme for non-diffuse holograms.

visibility (ratio of intensities in the light and dark areas) is much better using the reconstruction process and spurious patterns due to unintended reflections are avoided.

E. Background Pattern.

An important aid in the interpretation of interferograms is a linear pattern of fringes superimposed on the experimental pattern. The background helps in discerning shifts less than a wavelength which appear as departures from a straight line or it helps in complicated patterns to determine the order number of fringes. One sees in Fig. 16 interferograms of a gas stream with and without background fringes and the resulting ambiguity in the case without a background.

The background is introduced in a Mach Zender interferometer by tilting a mirror slightly. Similarly in double-exposure holographic interferometry a mirror can be tilted between the two exposures. To locate the fringes on the hologram plane (the

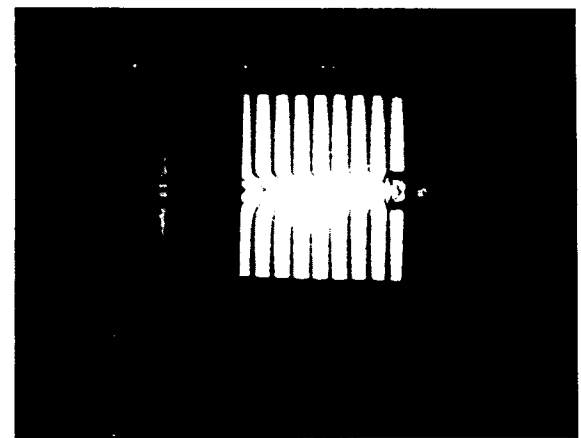
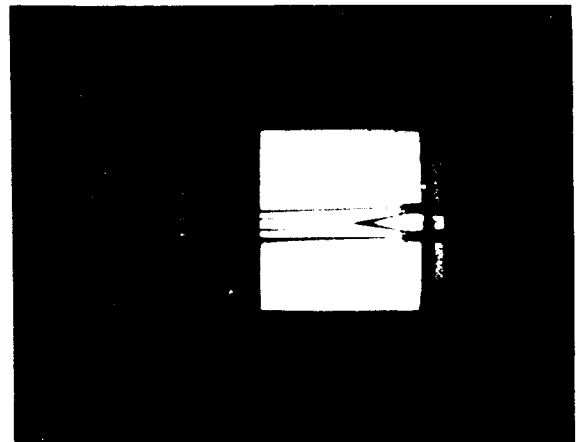


Fig. 16. Showing the significance of a background pattern to the interpretation of an interferogram.

same plane as the object of interest) it would be ideal to place a mirror at an image of the hologram, say in the reference beam. In practice we have found that unnecessary for the small amount of tilting actually used.

The mirror tilting is easily accomplished in a reproducible and remote way by heating a piece of wire as shown in Fig. 17. An AC current of about two amps in one-half inch of .015" diameter nichrome wire provides a few fringes per inch.

V. INTERPRETATION OF PLASMA INTERFEROGRAMS

Assuming the rays of the scene beam are arranged to be parallel (say to the z-axis), the basic measurement provides a two dimensional contour map of

$$N(x, y) = \int n_e(x, y, z) dz,$$

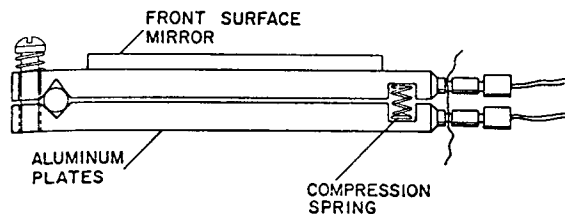


Fig. 17. A procedure for slightly tilting a mirror by heating a short piece of wire.

where as derived above the contours are in units of fringes and at 6943 Å

$$\text{Fringe shift} \times (3.2 \times 10^{17}) = \int n_e dz \text{ (cm}^{-2}\text{)}.$$

In speaking of fringe shifts it is assumed one correctly allows for the background pattern.

The simplest derived quantity is the total number of electrons in the field of view obtained by integrating over area. It should be noted that the number can be obtained with no knowledge of how n_e varies with z .

In simple situations the electron density can be observed along lines of constant density. The local density is then obtained by dividing the integrated measurement by length.

More complicated analysis, necessary when n_e is not constant along the line of sight, is still possible when there is some special symmetry. As an example we will describe the analysis of interferograms taken of a helical plasma.

Figure 18 shows schematically the shape of a helical $l = 1$ plasma column. The rays of the scene beam are parallel to the helical axis and therefore go in and out of the plasma column. In the actual experiment there were ten periods of helix so that the end-on view appeared cylindrically symmetric but represented a very distorted view of the plasma density.

The procedure chosen to analyse the interferogram was a non-linear least-squares fit of the data to curves representing a simple column which is helically distorted. A least-squares fit is particularly appropriate since the contour map provides only a finite number of points to represent the distribution. In this example, as with others such as Abel inversion, any procedure which re-

HELICAL $l=1$ PLASMA COLUMN

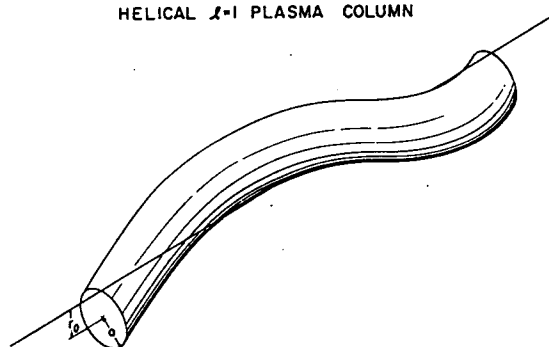


Fig. 18. The appearance of a helical $l = 1$ plasma column showing why parallel light rays go in and out of the plasma column.

quires computing from curves drawn through the raw data can generate surprising and significant errors in the final answer. The least-squares procedure avoids that problem although it can go wrong in various other ways. The essential step is to provide a reasonable set of parameters which have enough generality to fit the data but not so much freedom that the fitting procedure fails to converge.

Some of the details may be of interest. Interferograms such as those in Fig. 19 were examined by locating fringes along lines through the center of the distribution parallel and perpendicular to the background pattern. The fringe profile obtained perpendicular to the background contains a linear contribution due to the background. By examining the interferogram in regions where the fringes are not distorted by plasma it is easy to determine the linear contribution so it can be subtracted. The simplifying assumption made for the analysis was that the helically distorted column still had a simple cross-section in a plane perpendicular to the helical axis within which the density could be described by a gaussian times a power series in radius. The center of the distribution was assumed to follow a helical line located r_0 from the axis. With these assumptions the end-on profile of fringes can be calculated in terms of the various parameters and the least-squares fitting procedure was used to fix the parameters.

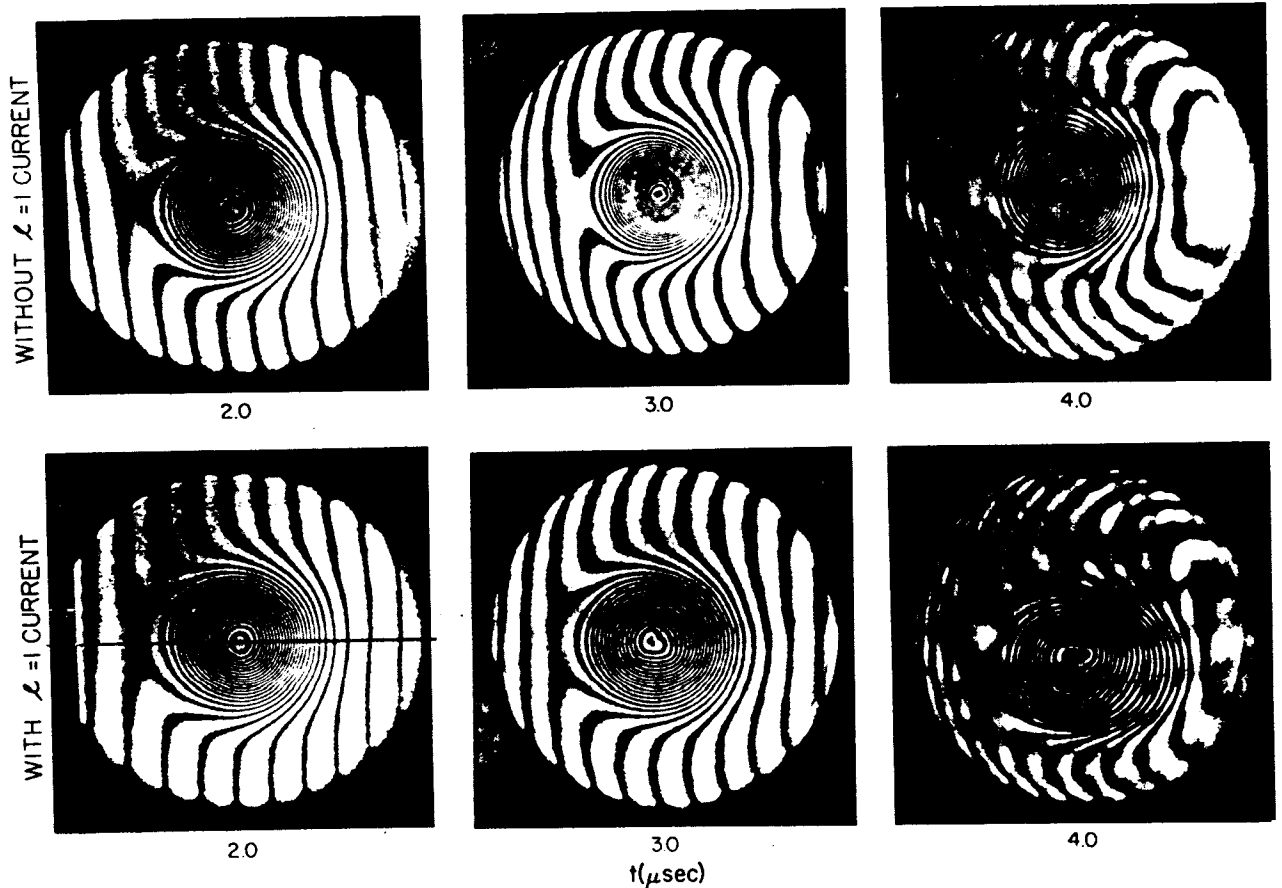


Fig. 19. Holographic interferograms made with and without helical fields.

Fig. 20 shows examples of fitted curves and the inferred local electron density profiles. One profile corresponds to a plasma shot with no applied helical ($l = 1$) fields and the other profile corresponds to a helically distorted plasma. Perhaps it is surprising that the two profiles could be discerned by the fitting procedure since they seem so similar at first glance. There are a number of reasons for this but the point of general interest is that the interferograms are quantitative and capable of very precise analysis.

Some comment is needed on the errors possible due to refractive effects. Density gradients can give rise to ray bending which complicates the interpretation of the fringe shift. An estimate of the effect in a particular experiment can be obtained from the leading order corrections calculated for a uniform density gradient.

$$\frac{\delta}{N} = \frac{l^2 e^2 \lambda^2}{24 \pi m c^2} \left(\frac{dn_e}{dx} \right)^2$$

where δ = the error in fringe number

N = the number of fringes

l = the length of the path through plasma

λ = the wavelength used

$\left(\frac{dn_e}{dx} \right)$ = the gradient of electron density perpendicular to the path of the ray

n_e = the electron density

$$\text{or } \frac{\delta}{N} = 1.8 \times 10^{-23} \frac{l^2}{n_e} \left(\frac{dn_e}{dx} \right)^2 \quad (\text{cgs})$$

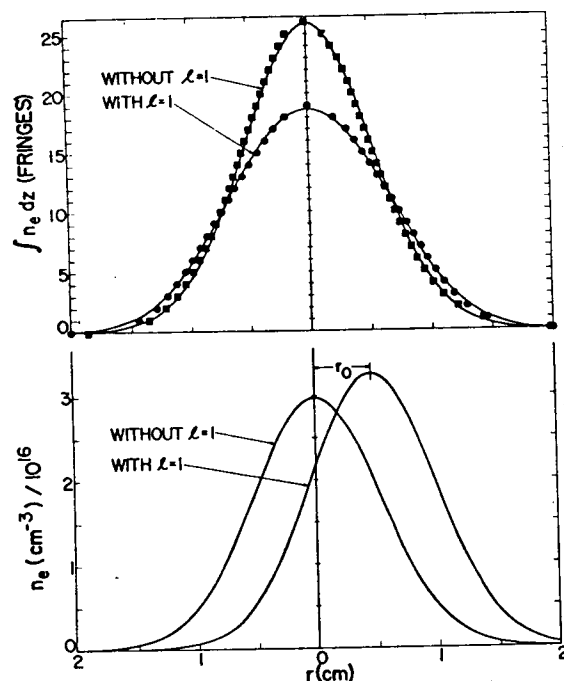


Fig. 20. Quantitative analysis of interferograms showing extraordinary agreement between data and theoretical treatment of helical distortion.

The error would be twice as large if there were not a lens to image the plasma onto the hologram plane. The reasoning is the same as that used in discussing poor windows. (see Fig. 8).

VI. ACKNOWLEDGMENTS

Our work in holographic interferometry started after receipt of a preprint of what has now become a classic paper in the literature: L. O. Heflinger, R. F. Wuerker, and R. E. Brooks, J. Appl. Phys. 37, 642 (1966). Upon recent rereading we were forcefully struck with how much of the work reported here is explicitly or implicitly foreshadowed there.

REFERENCES

1. F.C. Jahoda, et al., J. Appl. Phys. 35, 2351 (1964).
2. For example: H.M. Smith, Principles of Holography, Wiley-Interscience, 1969 or J. W. Goodman, Introduction to Fourier Optics, McGraw-Hill, 1968.
3. F.C. Jahoda, R.A. Jeffries, and G.A. Sawyer, Appl. Optics 6, 1407 (1967).
4. R. Sigel, Phys. Letters 30A, 103 (1969).
5. F.C. Jahoda, Appl. Phys. Letters 14, 341 (1969).
6. D.H. Close, A.D. Jacobson, J.D. Margerum, R.G. Brault, and F. J. McClung, Appl. Phys. Letters 14, 159 (1969).